Hindawi
Journal of Chemistry
Volume 2019, Article ID 3041097, 6 pages
https://doi.org/10.1155/2019/3041097

Research Article

Simulation Investigation on Flame Retardancy of the PVAc/ATP Nanocomposite

Su Qiong, Wang Yanbin, Liu Li, and Liang Junxi

Gansu Key Laboratory of Environmental Friendly Composites and Biomass Utilization, College of Chemical Engineering, Northwest Minzu University, Lanzhou, Gansu 730030, China

Correspondence should be addressed to Liang Junxi; xbmujxliang@126.com

Received 11 August 2018; Accepted 30 December 2018; Published 3 February 2019

Academic Editor: Ewa Schab-Balcerzak

Copyright © 2019 Su Qiong et al. This is an open access article distributed under the Creative Commons Attribution License, which permits unrestricted use, distribution, and reproduction in any medium, provided the original work is properly cited.

Molecular dynamics (MD) simulations were carried out to study the effects of some key factors on the enhancement of flame retardancy of the PVAc/ATP nanocomposite. As a result, the obvious improved flame retardancy was attributed mainly to the increased dispersion of Mg ions in the PVAc matrix due to the stronger interaction between PVAc and ATP and partially to the combustion temperature of PVAc released by the escaped H_2O originating from the ATP dopant. Hence, the ATP ore as a predicted additive is viewed as a prospective candidate to be applied in future organic materials to obtain better flame-retardant properties. Moreover, in our simulations, the temperature can induce a significant impact on the interaction of the PVAc/ATP nanocomposite, in which the prominent combination between PVAc and ATP could be greatly promoted at 350 K.

1. Introduction

Poly(vinyl acetate) (PVAc) is often used for coating the porous materials; however, the flammability quite limits its wide applications, such as wood processing, fabric bonding, furniture assemble, packaging materials, and building decoration [1]. In general, flame-retardant polymer-based materials are prepared by blending the polymer matrix with some appropriate additives, such as organic bromides, red phosphorus, magnesium hydroxide, and aluminum hydroxide [2]. Known to possess rich sources and environmentally friendly features, the nanofillers and their derivatives, e.g., clays, are being considered as a promising alternative for the conventional additives to be used in the synthesis of nanocomposites with high flame retardancy [3, 4]. Recently, studies show that prepared polylactic acid (PLA) added to a small amount of attapulgite (ATP) ores can overcome some of its own negative effects, such as low melt viscosity, low heat distortion temperature, and bad gas barrier, and thereby favorably develop its applications in various fields [5–10]. Nevertheless, in their research, a question is how to achieve the flame retardancy that was poorly understood and remaining a great challenge. Because of the presence of some required flame-retardant factors, such as moisture and metals, [11] the cheap ATP ores can emerge as a good and potential additive for the PVAc to prepare the high flame-retardant hybrid materials. With this in mind, we assume that if the PVAc contains some metal atoms and H_2O molecules released from the ATP, in turn, the surface of the PVAc may trap more degradation products during combustion. As a result, the corresponding thermal stability and even flame retardancy can be improved. To test these hypotheses, the effects of the interaction between PVAc and ATP on the flame-retardant materials should be studied in detail. However, it is particularly difficult to monitor the possible movement of the released metal atoms and H_2O molecules inside the PVAc/ATP composite; henceforth, a computational simulation technique has to be employed [12, 13]. In this article, our attention was focused on the investigation of interfacial interaction between the tested ATP and PVAc by means of atomistic classical molecular dynamics (MD) to predict the dynamics of the available Mg ions and H_2O molecules from ATP at different temperatures. It is hoped that our studies provide some information and descriptions for the explanation of the flame retardancy of PVAc/ATP

composites, which can be an important and effective method to significantly expand PVAc applications in future.

2. Materials and Methods

2.1. Model Building. As the PVAc is a large and complex polymer [14], it is difficult to model it normally. Hence, in this paper, the relatively low polymerization degree of PVAc is used rationally, where the defined PVAc macromolecule consisting of 250 vinyl acetate units is constructed and the end groups are saturated by two H atoms. This assumption is well similar to the investigation of Zhou and coworkers [15], who have reported the model of polylactic acid with 100 predicted polymerization degrees, and the corresponding characters after simulation could meet the requirements such as research precision. With the above exposures, an initial model of PVAc at a density of 1.07 g·cm^{-3} is obtained by an amorphous cell module on the optimized geometry completed by using the Forcite module. On the other hand, according to the experimental results from heat treatment [16, 17], the orthorhombic ATP crystal [18] cell with the (100) surface has been constructed. At last, as observed from Figure 1(a), the PVAc-ATP (100) interface interaction was built by setting up the above-established PVAc and ATP cells assembled together using the "build layers" command of the Material Studio (MS) software, in which the box size is 1.79 nm × 1.57 nm × 11.84 nm and the density for the system is 1.30 g·cm^{-3}.

2.2. Simulation Methods. Starting from the PVAc-ATP minimized structure performed by the smart minimizer method, MD simulation was subsequently carried out at a temperature of 300, 350, and 400 K at a pressure of 100 MPa employed by the Andersen thermostat method [19], in which NVT ensemble balance was conducted to the system with the COMPASS force field [20] and a fixed time step of 1 fs was used. Moreover, the equations of motion for the molecules were integrated using the Verlet leapfrog scheme [21], and Coulomb and van der Waals long-range, nonbonded interactions were handled by using the standard Ewald and atom-based summation methods, respectively [22]. All simulations are performed by using the Forcite module [23].

3. Results and Discussion

3.1. Equilibrium Configuration. Shapes of the PVAc/ATP geometries obtained at the three different temperatures 300, 350, and 400 K, respectively, have been given vividly in Figure 1. At the same time, the initial building PVAc/ATP configuration (Figure 1(a)) is also presented for comparison purposes. Compared to the starting configuration, it is clear that configurations of the simulated PVAc under different temperatures are very similar to each other, displaying cluster together visibly. This means the effect of the temperature on the structure of PVAc is little. More intriguingly, with the temperature increasing, the structure of ATP becomes incompact, diplaying more relaxation, with respect to that found for the PVAc. The features favor formation of the network-like structure around PVAc [24], which can hinder the movement of polymer chains and thus help to improve flame retardancy. Figure 1 also reveals that the temperature causes an effect that is responsible for the types and amounts of the components diffusing from the ATP, which differs from the observed cases at 300 K (diffusion of some Mg and O). Our present simulations illustrate that abundant Mg^{2+} ions and some H_2O molecules apparently diffuse at both 350 K and 400 K.

It is also worth highlighting that, at any temperature presented in this paper, the behaviour of Mg ions diffusing from the ATP to PVAc takes place uniformly and dramatically, which is a very crucial factor for remarkable improvement in flame retardancy of the polymers [25, 26]. This might give us a reasonable explanation why the composite of PVAc/ATP is found to have less flammability than the original PVAc material. Nevertheless, our simulation results of the PVAc/ATP composite at 300 K, giving rise to diffusion of O atoms marked blue in the simulation cell (see Figure 1(b)), shed light into its increased flammability compared to the pure PVAc polymer. In contrast, with increasing the temperature, the diffusion of the H_2O molecules in preference to oxygen cases from the ATP to the PVAc leads to the peak heat release rate reduction of nanocomposite, in which capability of the corresponding flame retardancy is greatly promoted. Consequently, the influence of temperature on the composite material of PVAc/ATP with favorable flame retardancy becomes predominant.

3.2. Relationship between Interaction and Temperature. Discussion of the interface interaction of the PVAc/ATP composite may be a key issue to elucidate the diffusion degree of Mg ions coming from ATP within the PVAc, favoring improvement in the flame retardancy of polymers; however, this associated effect is often affected by the temperature. Therefore, an analysis of the relationship between interaction and temperature is very important and indispensable. In this paper, the molecular interaction can be evaluated by binding energies (E_{bind}), and the corresponding computed values are summarized in Table 1. Here, the E_{bind} is defined as the negative of the adsorption energy ($E_{\text{adsorption}}$). The $E_{\text{adsorption}}$ between the PVAc and the ATP is calculated by using the following equation:

$$E_{\text{adsorption}} = E_{\text{total}} - \left(E_{\text{PVAc}} + E_{\text{ATP}}\right), \quad (1)$$

where E_{total}, E_{PVAc}, and E_{ATP} represent the potential energies of the PVAc/ATP composite, PVAc, and ATP systems, respectively.

Compared to the relationship between E_{bind} and temperature (Table 1), the most remarkable finding is 4310.58, 5844.75, and 4454.29 kcal·mol^{-1} at the temperatures 300, 350, and 400 K, respectively, indicating the possibility of PVAc having a more stable interaction towards the ATP surface [27]. Of course, of the temperatures considered here, values of the stated $E_{\text{adsorption}}$ must be negative; hence, it implies that the ATP acted as an excellent additive. Obviously, since the interaction is benefiting from the good dispersion of Mg ions, the incorporated ATP improves flame retardancy of the nanocomposites. This result is

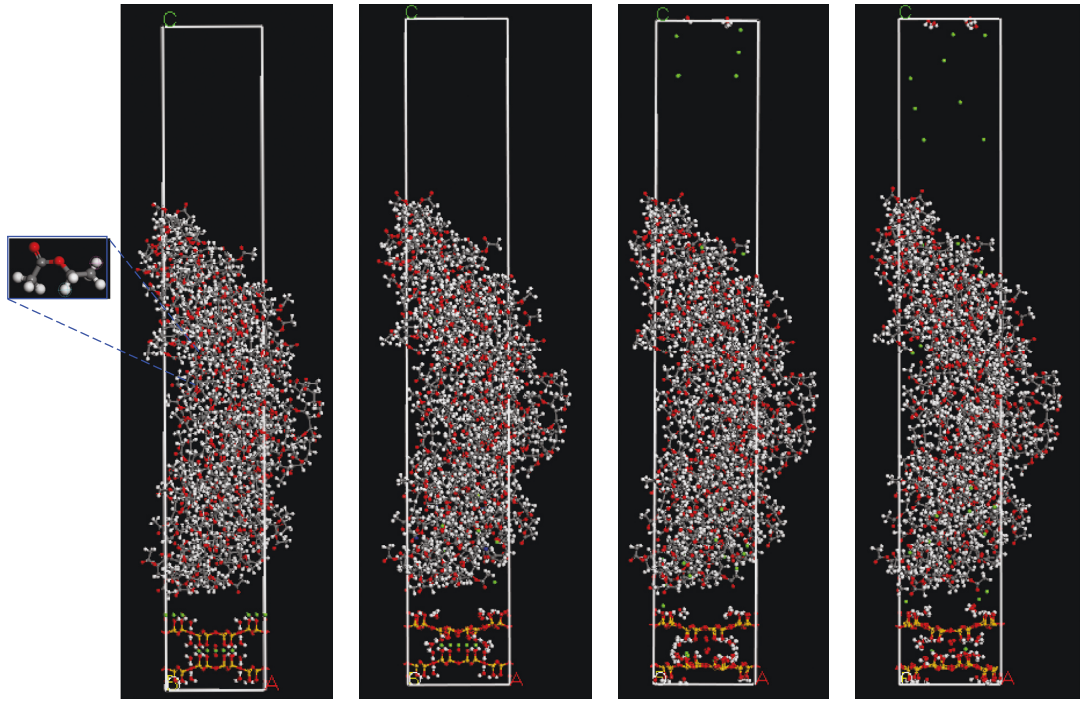

Figure 1: Configurations for the interaction of PVAc with the ATP (100) surface. (a) Initial building configuration; (b), (c), and (d) equilibrium configurations obtained at a temperature of 300, 350, and 400 K, respectively. Here, the oxygen atoms which escaped from ATP to PVAc are shown in blue.

Table 1: Some important parameters for evaluating flame retardancy of the PVAc/ATP nanocomposite. The symbols E_{bind}, D_{Mg}, and FFV represent binding energies, Mg^{2+} diffusion coefficient, and fractional free volume, respectively.

Temperature (K)	300	350	400
E_{bind} (kcal·mol^{-1})	4310.58	5844.75	4454.29
D_{Mg} (cm^2·s^{-1})	6.33×10^{-4}	2.45×10^{-4}	2.71×10^{-4}
FFV (%)	36.96	35.71	35.81
Surface area (Å^2)	2177.31	2472.39	2589.31

already confirmed by configurations of the abovementioned optimized complexes. As can be seen from Figure 1, many relaxed Mg ions from the ATP strongly diffuse away to the PVAc. Moreover, it is also evident that the temperature can induce a significant impact on the interaction between PVAc and ATP. However, the characterized observation also shows that higher temperature does not correlate with stronger interaction; e.g., the largest E_{bind} appears at 350 K. That is, the study of E_{bind} leads us to infer the possibility of the interaction between PVAc and ATP being relatively more selective towards temperature.

3.3. Relationship between Diffusion and Temperature. To clearly gain deeper insights into the characteristics of flame retardancy of the PVAc/ATP nanocomposite, analysis of the relationship between diffusion and temperature is most important, and so in this paper, investigations of Mg-diffusion behaviour were performed at 300, 350, and 400 K.

3.3.1. Mean Square Displacement (MSD). As a vital factor for improvement of the flame retardancy, the mobility of Mg ions inside the PVAc is highly key and generally assessed by computing the diffusion coefficient (D) [28]. The relationship between MSDs with time is plotted in Figure 2. The corresponding computed values of D for Mg ions at different temperatures are reported in Table 1. The results show that MSD of the Mg ions through D expression decreases as the temperature (K) increases from 300 to 350 to 400. However, when the temperature is at either 350 or 400 K, as the result is clear from the simulation shown in Figure 2, a fairly linear correlation between MSD and time identically occurs, implying the Mg ions may be dispersed well in the PVAc matrix. So, the flame-retardant mechanism of the addition of ATP particles to PVAc, as a barrier for degradation products as already stated in Section 1, was to be the coagulation and accumulation of loose Mg ions near the PVAc surface to form a protective layer as a heat insulation. This speculation will be fully confirmed by the radial distribution functions (RDFs), and the detailed elucidations are given in Section 3.3.2. In addition, although the D_{Mg} values (cm^2·s^{-1}) are of the same order of magnitude, displaying 6.33×10^{-4} (300 K), 2.45×10^{-4} (350 K), and 2.71×10^{-4} (400 K), the coefficient is relatively larger when the temperature is equal to 300 K. This result is not surprising because at 300 K, the Mg ions diffuse from ATP, accompanied by some polar O atom diffusion. Also, the counterpart D_{Mg} at 350 K displays smaller values than that at 400 K, corroborating that the movement of Mg ions from ATP is hindered, thanks to the severe physical barrier effect

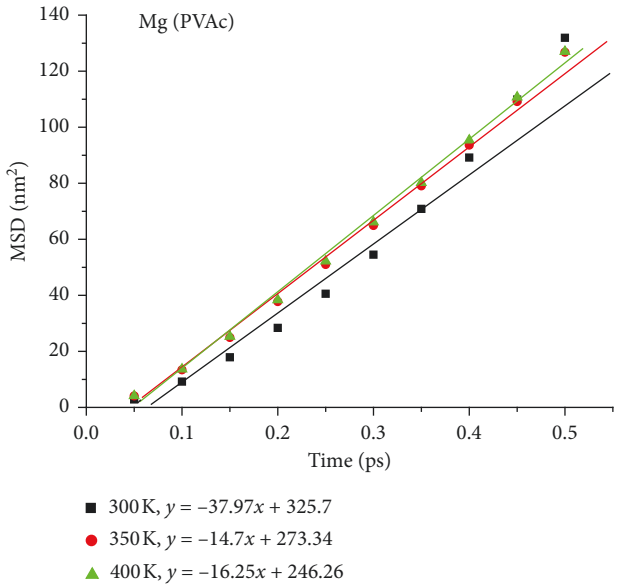

Figure 2: The relationship between MSD and time with temperature increasing. Each color is associated with different temperatures.

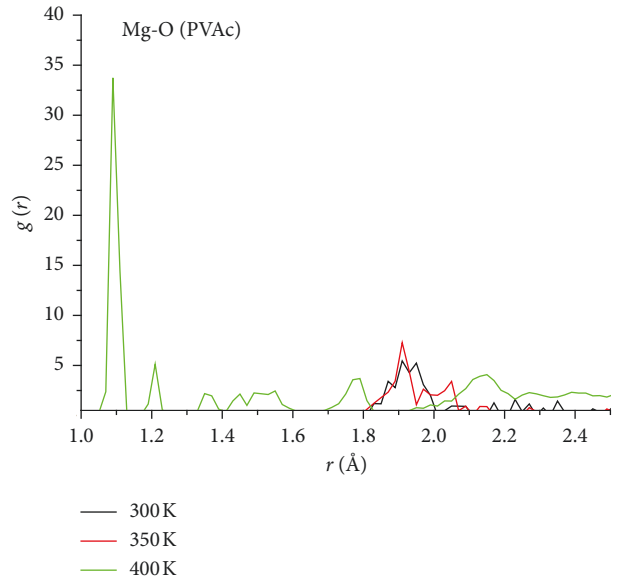

Figure 3: Mg-Poly pinpoints main relevant features in pair RDFs. Each color is associated with different temperatures.

derived from the stronger interface interaction [29–31], and thus slows down the Mg diffusion within PVAc. These are well inferred by the fractional free volume (FFV, %) of PVAc/ATP, indicating the order 36.96 (300 K) > 35.81 (400 K) > 35.71 (350 K), as shown in Table 1. Therefore, with temperature increasing, flame-retardant efficiency of the composite of PVAc/ATP seems to not increase.

3.3.2. Radial Distribution Functions (RDFs). To further determine pronounced differences of Mg ions near the PVAc surface because of the temperature change, the RDFs of Mg-O(PVAc) were calculated. As can be seen from Figure 3, our simulations show that, at 400 K, the highest peak of $g(r)$ for Mg was located at 1.05–1.14 Å, while at the remaining two, 300 K and 350 K, the corresponding peaks are observed within the 1.80–2.10 Å distance range, and the obtained peak positions and shapes do not greatly differ. Since then, the orientations of Mg ions around PVAc is abundant at 400 K; in comparison, in particular, the acute intensity of the peak indicates the enormous coagulation of Mg ions on the PVAc surface and thus favors improving flame retardancy of the PVAc. This speculation is fully supported by Mg ions around the surface area (Å^2) of the PVAc/ATP, such as 2177.31 (300 K) < 2472.39 (350 K) < 2589.31 (400 K) as listed in Table 1. It should be noted that, as shown in Figure 3, at both 300 K and 350 K, the distance ranges (1.80–2.10 Å) with the peak of $g(r)$ for Mg are less than the ion distances (2.13 Å) of the isolated MgO molecule [32, 33], especially at 400 K (1.05–1.14 Å), which possibly facilitates very strong Mg-O(PVAc) interactions. Such a match between the Mg-O(PVAc) and Mg-O distances has a remarkable impact on the coagulation of Mg ions around the PVAc. This is also the most plausible reason to explain the less flammability of the PVAc/ATP composite material.

3.3.3. Atomic Density Profiles. Density profiles of the Mg ions near the PVAc surface can provide some available evidence for understanding how the flame retardancy of PVAc/ATP is affected by the presence of Mg. Figure 4 illustrates the plots for the density of Mg ions inside the PVAc/ATP composite, in which the profile is parallel to the z-axis and normal to the ATP (100) surface. Based on the analysis of the density map, it is clear from our results that, for the different temperatures considered here, two notable peaks located at 20 Å and 55 Å within the range were revealed and the corresponding examined magnitude obeys the order of 300 K > 400 K > 350 K. The relatively high peaks in the Mg^{2+} concentration occurring at 300 K indicate that Mg ions have been evenly distributed inside the PVAc/ATP composite under room temperature. Moreover, at approximately 5 and 80 Å, the other two distinct peaks were situated as well but only for both 350 and 400 K, in which the peak values at different orientations are associated with temperature. Obviously, with the temperature increasing, the diffuse Mg ions can freely reorient on the PVAc/ATP surface. Nevertheless, at higher temperature, Mg ions diffuse to the PVAc/ATP surface with no preferred orientation, inferring some facing up into the vacuum space (see Figure 1). Therefore, in conjunction with the RDF results, one may speculate that high temperature can preferentially fix Mg coagulation around the PVAc surface, thus improving the flame retardancy.

3.4. Experimental Results. Flame-retardant performance of the original PVAc emulsion and PVAc blended with 0.01% acidulated ATP ores is measured through combustion occurring on the paper substrate, in which two preferred tests, horizontal and vertical, were accomplished, respectively. Here, the phenomenon of less agglomerate and more effective dispersal was found for the 0.01% ATP-dopant mixed inside the PVAc emulsion. The obtained results are summarized in Table 2. It can be seen from this table that the

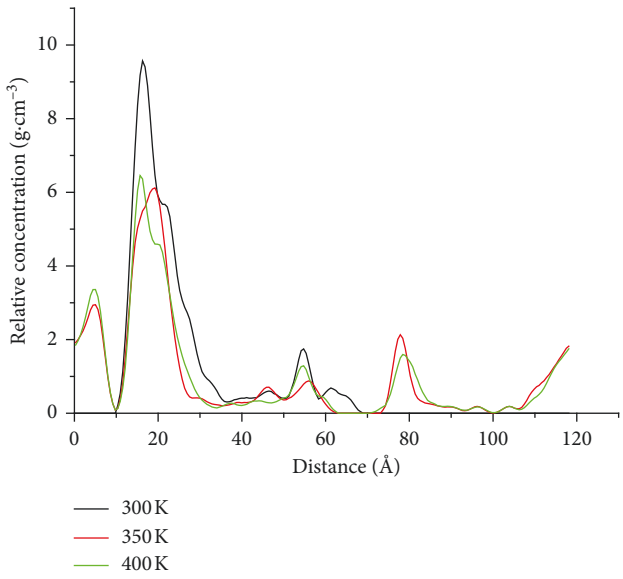

Figure 4: With temperature increasing, the concentration of Mg ions inside the PVAc/ATP is a function of the distance z (far from the bottom of the simulation cell) perpendicular to the surface. Each color is associated with different temperatures.

Table 2: Results of flame-retardant performance tested on the paper.

Type	Sample	Afterflame time (s)	Afterglow time (s)
Horizontal test	PVAc/ATP	45	41
	PVAc	50	44
Vertical test	PVAc/ATP	39	41
	PVAc	44	44

paper covered with PVAc/ATP has shorter combustion times (either afterflame or afterglow times) than that with pure PVAc, which is in accordance with the results of favorable flame retardancy for the composite of PVAc/ATP. Moreover, taking the horizontal test on the paper with PVAc/ATP in comparison to the PVAc case as an example, there are 5s and 3s times decreases for the afterflame and afterglow combustions, respectively; the vertical test is analogous. Obviously, under the afterflame condition, the flame retardant efficiency of the PVAc/ATP composite increases, supporting the great influence of temperature on flame retardancy, i.e., the higher the temperature, the more obvious the efficiency is. These further validate our molecular modeling computations.

4. Concluding Remarks

In this paper, the flame retardancy of a novel PVAc-based nanocomposite prepared by a cheap additive ATP in a PVAc matrix has been studied using the MD method. Compared to the original PVAc, the as-fabricated nanocomposite exhibits significantly enhanced flame retardancy. Because of the stronger interfacial interaction between PVAc and ATP, the better dispersion of Mg ions plays a key role in the enhancement of flame retardancy of the nanocomposite, which is well consistent with the experimental observation. The bestowed results in this study bring to light the mechanism for finding ATP flame retardancy in PVAc polymers, proposing that nano-ATP ores emerge as realistic and auspicious alternatives for the conventional flame retardants currently used.

Data Availability

The data used to support the findings of this study are available from the corresponding author upon request.

Conflicts of Interest

The authors declare that there are no conflicts of interest regarding the publication of this paper.

Acknowledgments

This study was supported by the Natural Science Foundation of China (51563022), Undergraduate Teaching Construction Project of Northwest Minzu University: Comprehensive Reform Pilot of Chemical Engineering and Technology Specialty (2017XJZYZH GGSD-03), and Fundamental Research Funds for the Central Universities (zyp2015018).

References

[1] E. Burdurle, Y. Kilic, G. C. Elibol, and M. Kilic, "The shear strength of Calabrian pine (*Pinus brutia* Ten.) bonded with polyurethane and polyvinyl acetate adhesives," *Journal of Applied Polymer Science*, vol. 99, no. 6, pp. 3050–3061, 2006.

[2] A. Dasari, Z.-Z. Yu, G.-P. Cai, and Y.-W. Mai, "Recent developments in the fire retardancy of polymeric materials," *Progress in Polymer Science*, vol. 38, no. 9, pp. 1357–1387, 2013.

[3] Y.-C. Li, J. Schulz, S. Mannen et al., "Flame retardant behavior of polyelectrolyte–clay thin film assemblies on cotton fabric," *ACS Nano*, vol. 4, no. 6, pp. 3325–3337, 2010.

[4] S. Chen, X. Li, Y. Li, and J. Sun, "Intumescent flame-retardant and self-healing superhydrophobic coatings on cotton fabric," *ACS Nano*, vol. 9, no. 4, pp. 4070–076, 2015.

[5] P. Emilie, E. Eliane, and F. René, "Effect of an organo-modified montmorillonite on PLA crystallization and gas barrier properties," *Applied Clay Science*, vol. 53, no. 1, pp. 58–65, 2011.

[6] S.-S. Ray, K. Yamada, M. Okamoto, A. Ogami, and K. Ueda, "New polylactide/layered silicate nanocomposites. 3. High-performance biodegradable materials," *Chemistry of Materials*, vol. 15, no. 7, pp. 1456–1465, 2003.

[7] M.-A. Paul, M. Alexandre, P. Degée, C. Henrist, A. Rulmont, and P. Dubois, "New nanocomposite materials based on plasticized poly(l-lactide) and organo-modified montmorillonites: thermal and morphological study," *Polymer*, vol. 44, no. 2, pp. 443–450, 2003.

[8] K. Fukushima, D. Tabuani, and G. Camino, "Nanocomposites of PLA and PCL based on montmorillonite and sepiolite," *Materials Science and Engineering: C*, vol. 29, no. 4, pp. 1433–1441, 2009.

[9] M. Murariu, L. Bonnaud, P. Yoann, G. Fontaine, S. Bourbigot, and P. Dubois, "New trends in polylactide (PLA)-based materials: "Green" PLA-Calcium sulfate (nano)composites tailored with flame retardant properties," *Polymer Degradation and Stability*, vol. 95, no. 3, pp. 374–381, 2010.

[10] L. Jiang, J. Zhang, and M. P. Wolcott, "Comparison of polylactide/nano-sized calcium carbonate and polylactide/montmorillonite composites: reinforcing effects and toughening mechanisms," *Polymer*, vol. 48, no. 26, pp. 7632–7644, 2007.

[11] B. Xu, W. M. Huang, Y. T. Pei et al., "Mechanical properties of attapulgite clay reinforced polyurethane shape-memory nanocomposites," *European Polymer Journal*, vol. 45, no. 7, pp. 1904–1911, 2009.

[12] R. Kumar, R. N. Shinde, D. Ajay, and M. E. Sobhia, "Probing interaction requirements in PTP1B inhibitors: a comparative molecular dynamics study," *Journal of Chemical Information and Modeling*, vol. 50, no. 6, pp. 1147–1158, 2010.

[13] R. Tosaka, H. Yamamoto, I. Ohdomari, and T. Watanabe, "Adsorption mechanism of ribosomal protein L2 onto a silica surface: a molecular dynamics simulation study," *Langmuir*, vol. 26, no. 12, pp. 9950–9955, 2010.

[14] R. P. D'Amelia and H. Jacin, "Characterization of low molecular weight polyvinyl acetate," *Industrial and Engineering Chemistry Product Research and Development*, vol. 15, no. 4, pp. 303–307, 1976.

[15] S.-Q. Zhou, X.-C. Cheng, Y.-L. Jin, J. Wu, and D.-S. Zhao, "Molecular dynamics simulation on interacting and mechanical properties of polylactic acid and attapulgite(100) surface," *Journal of Applied Polymer Science*, vol. 128, no. 5, pp. 3043–3049, 2012.

[16] J. E. Post and P. J. Heaney, "Synchrotron powder X-ray diffraction study of the structure and dehydration behavior of palygorskite," *American Mineralogist*, vol. 93, no. 4, pp. 667–675, 2008.

[17] R. Giustetto and G. Chiari, "Crystal structure refinement of palygorskite from neutron powder diffraction," *European Journal of Mineralogy*, vol. 16, no. 3, pp. 521–532, 2004.

[18] J.-E. Chisholm, "Powder-diffraction patterns and structural models for palygorskite," *The Canadian Mineralogist*, vol. 30, p. 61, 1992.

[19] H. C. Andersen, "Molecular dynamics simulations at constant pressure and/or temperature," *Journal of Chemical Physics*, vol. 72, no. 4, pp. 2384–2393, 1980.

[20] H. Sun, "COMPASS: an ab initio force-field optimized for condensed-phase ApplicationsOverview with details on alkane and benzene compounds," *Journal of Physical Chemistry B*, vol. 102, no. 38, pp. 7338–7364, 1998.

[21] M.-P. Allen and D.-J. Tildesley, *Computer Simulation of Liquids*, Clarendon Press (Hardback edition), Oxford, UK, 1987.

[22] J.-P. Hansen and I.-R. McDonald, *Theory of Simple Liquids*, Academic Press, London, UK, 2nd edition, 1990.

[23] A. Górecki, M. Szypowski, M. Dlugosz, and J. Trylska, "RedMD-reduced molecular dynamics package," *Journal of Computational Chemistry*, vol. 30, no. 14, p. 2364, 2009.

[24] H. Ma, L. Tong, Z. Xu, and Z. Fang, "Synergistic effect of carbon nanotube and clay for improving the flame retardancy of ABS resin," *Nanotechnology*, vol. 18, no. 37, p. 375602, 2007.

[25] C. Bao, Y. Guo, B. Yuan, Y. Hu, and L. Song, "Functionalized graphene oxide for fire safety applications of polymers: a combination of condensed phase flame retardant strategies," *Journal of Materials Chemistry*, vol. 22, no. 43, p. 23057, 2012.

[26] P. Kiliaris and C. D. Papaspyrides, "Polymer/layered silicate (clay) nanocomposites: an overview of flame retardancy," *Progress in Polymer Science*, vol. 35, no. 7, pp. 902–958, 2010.

[27] B. Li, S.-Y. Liu, M.-Q. Fan, and L. Zhang, "Interfacial water at the low-rank coal surface: an experiment and simulation study," *Theoretical Chemistry Accounts*, vol. 137, no. 6, p. 81, 2018.

[28] M. Meunier, "Diffusion coefficients of small gas molecules in amorphous cis-1,4-polybutadiene estimated by molecular dynamics simulations," *Journal of Chemical Physics*, vol. 123, no. 13, article 134906, 2005.

[29] C. Bao, L. Song, C. A. Wilkie et al., "Graphite oxide, graphene, and metal-loaded graphene for fire safety applications of polystyrene," *Journal of Materials Chemistry*, vol. 22, no. 32, p. 16399, 2012.

[30] K. Zhou, S. Jiang, C. Bao et al., "Preparation of poly(vinyl alcohol) nanocomposites with molybdenum disulfide (MoS2): structural characteristics and markedly enhanced properties," *RSC Advances*, vol. 2, no. 31, p. 11695, 2012.

[31] Z. Matusinovic, R. Shukla, E. Manias, C. G. Hogshead, and C. A. Wilkie, "Polystyrene/molybdenum disulfide and poly(-methyl methacrylate)/molybdenum disulfide nanocomposites with enhanced thermal stability," *Polymer Degradation and Stability*, vol. 97, no. 12, pp. 2481–2486, 2012.

[32] M.-J. Malliavin and C. Coudray, "Ab initiocalculations on (MgO)n, (CaO)n, and (NaCl)nclusters (n=1-6)," *The Journal of Chemical Physics*, vol. 106, no. 6, pp. 2323–2330, 1997.

[33] S. Moukouri and C. Noguera, "Theoretical study of small MgO clusters," *Zeitschrift für Physik D Atoms, Molecules and Clusters*, vol. 24, no. 1, pp. 71–79, 1992.

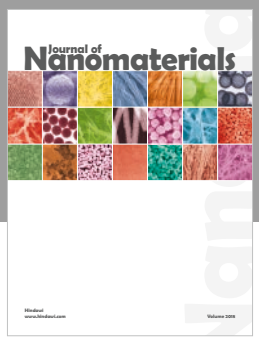

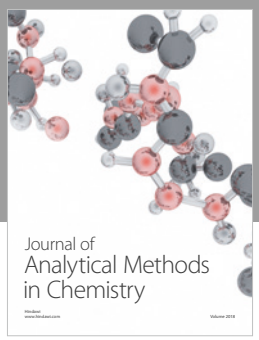

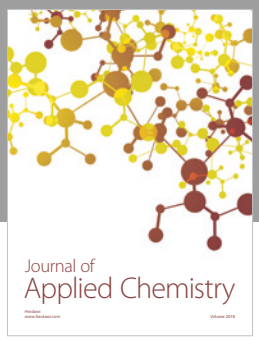

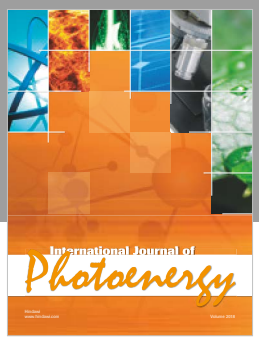

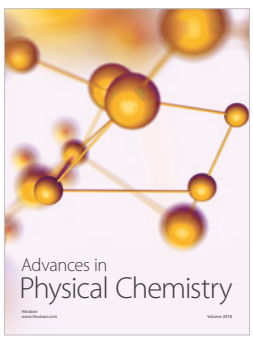

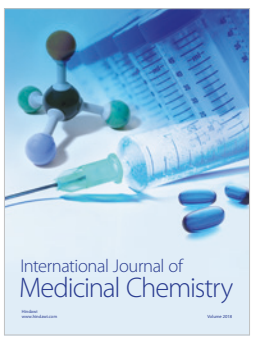

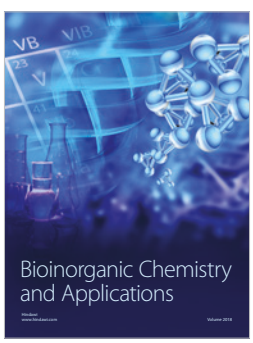

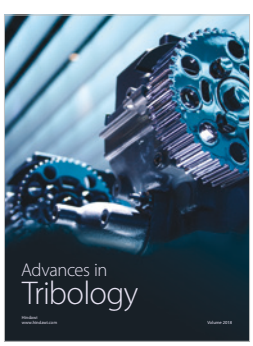

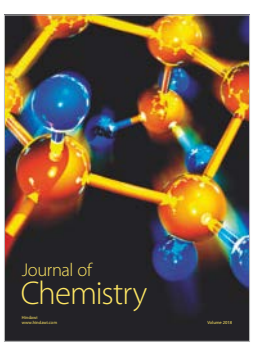

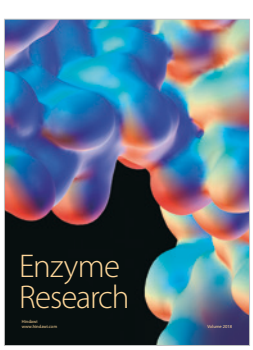

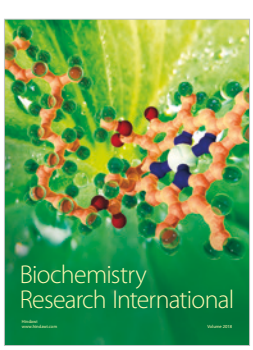

Hindawi

Submit your manuscripts at
www.hindawi.com